INTERNATIONAL JOURNAL OF CONSERVATION SCIENCE

ISSN: 2067-533X Volume 13, Issue 1, January-March 2022: 43-56 www.ijcs.ro

ELECTROCHEMICAL COMPARISON OF PHENOLIC ANTIOXIDANTS IN CONSERVATION OF IRON GALL INK PAPERS

Mohammad HADADI [1], Maryam AFSHARPOUR [2],
Mehrnaz AZADI-BOYAGHCHI [1], Meisam SADEGHI [3,*]

[1] Department of Conservation of Cultural and Historical Properties, Conservation & Restoration Faculty, Art University of Isfahan, 1744, Isfahan, Iran
[2] Department of Inorganic Chemistry, Chemistry and Chemical Engineering Research Center of Iran, CCERCI, 14335-186 Tehran, Iran
[3] Nanotechnology Research Institute of Mazandaran, Faculty of Chemical Engineering, Babol Noshirvani University of Technology, Babol, Iran

Abstract

Electrochemical behavior of three synthetic antioxidants, Butylated hydroxyltoluene (BHT), Butylated hydroxylanisole (BHA), and tert-Butyl hydroquinone (TBHQ) was researched by differential pulse voltammetry (DPV) technique on carbon paste electrode (CPE). According to this, a new method for the simultaneous determination of BHA, BHT, and TBHQ alone or in their mixtures was developed in order to obtain optimum concentration antioxidants against "ink corrosion" phenomenon in the iron gall inked papers. DPV can be used for quantitative data determination and also analysis studies on the kinetics, thermodynamics and mechanism of electrochemical reaction parameters. The voltammetric peaks of these antioxidants show well-defined and separated oxidation peaks based on their oxidation of BHA, BHT, and TBHQ. The proposed procedure is to provide a relationship between the peak current and analyte concentration. In addition, we found that during the redox reactions of TBHQ, BHA, and BHT, the redox peak currents increased and peak potentials highly shifted that these conditions can be attributed to the advantages of their strongly electro-active electrode. More results suggest that they have the same oxidation products. The obtained results indicate the sensitive, precise, and accurate method that can be an analytical alternative for existing methods.

***Keywords**: Antioxidant activity; Differential pulse voltammetry; Ink corrosion; Oxidation peaks; Optimum concentration.*

Introduction

The most important information carriers in the history of humankind as drawing and writing support are Papers. In libraries and archives, paper mainly made up of the cellulose as a most prominent structural component [1, 2]. Cellulose is often severe damaged by the writing media used, especially iron gall ink corrosion or copper pigments [3-6]. Generally, iron gall ink was a mixture of vitriol, a liquid carrier, gall tannins and a viscous additive such as Arabic gum [7, 8]. A serious problem is present of damaged archival documents with this ink. This degradation phenomenon is commonly known as the iron gall "ink burn" or "ink corrosion". Thus, due to the extensive degree of damage caused by ink corrosion under unfavorable

---

[*] Corresponding author: meisam_sadeghi1363@yahoo.com

environmental conditions, feeling that there is an urgent need for the conservation of objects made iron gall ink [9, 10].

Characteristics of the corrosive iron gall ink are a current issue in the conservation field. Unfortunately, corrosion of the substrate is revealed by diffusion of the color into the surroundings of the letters and ink penetration through cracks that leading to loss of the parts of the paper with the writing [11]. Observations on Current paper showed that most part of the brown stains formed around the ink lines are a common effect [11-14]. Degradation produced by iron gall inks containing paper is an important factor caused by many effects such as the ink applied, the paper thickness and the paper support [12].

Acids and transition metals were detected as relatively high contents of historical iron gall inks. Hence, hydrolysis and oxidation of cellulose have been identified as two main points for the preservation of these papers due to decay causes a decrease in paper strength. Fortunately, degradation pathways of ink corrosion often act in synergism [5, 6, 15-17]. At the molecular level, the oxidation reactions result in formation of carboxyl or carbonyl groups and cellulose enzymatic hydrolysis causing the changes in the length of cellulose chains. Consequently, at the macroscopic scale, the oxidative degradation leads to a yellow to brown color effect on paper and mechanical losses. Therefore, in order to achieve the result, both of pathways should be slowed down. Today's, antioxidants are engaged to prevent imperceptible degradation of the paper [18].

Due to the role of antioxidants in degradation processes, different types of antioxidants have been employed and some have been applied for this purpose [19]. Electrochemical methods get the possible potential for the investigation of various antioxidant measurements. Therefore, electrodes can be used for the testing purposes [20]. A typical electrochemical cell consists of three electrodes: (i) the most commonly used reference electrodes for aqueous solutions are the Ag/AgCl electrode, (ii) most often the counter electrode consists of a thin Pt wire, and (iii) the working electrodes are of various geometries and materials, ranging from gold and platinum to glassy carbon.

Based on this study, the electrochemical analysis carries out using differential pulse voltammetry (DPV) technique [21]. DPV method is effective, rapid, and modern electro-analytical technique possessed advantages such as Successful discrimination, low detection limits and low background current effect [22]. In this method, the scanning strategy uses a fixed series of potential. For each pulse, current is measured at the first and final of each pulse and the difference is calculated and plotted versus base potential [23-25]. The aim objective of this study was evaluation of a various antioxidant effects on the stability of papers comprising iron gall ink treatment against corrosion in order to obtain optimum concentration antioxidants against “ink corrosion” phenomenon. Despite the great number of antioxidant compounds available, only a few are used in the food industry [26]. In this work, the three kinds of antioxidant used in the food industry, BHA, BHT, and TBHQ was studied and applied.

Experimental part

Materials

All used chemicals were purchased from Merck, Fluka and Sigma-Aldrich. Distilled water and ethanol buffer solution with different pH values were provided. This CPE is composed of High viscosity paraffin (d = 0.88kg·L^{-1}) and pure graphite powders which prepared as the pasting liquid and substrate, respectively. The antioxidants used were BHA (98.50%), BHT (99%), and TBHQ (97%).The structures of the antioxidants are exhibited in Figure 1.

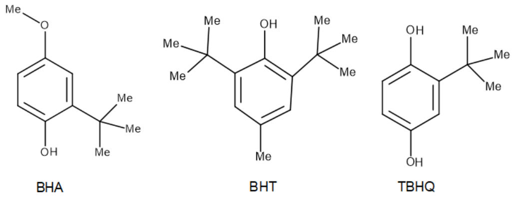

Fig. 1. Chemical structures of the phenolic antioxidants

The products formed of BHA and TBHQ obtained at a CPE have been presented in part (a). The authors propose that the oxidative product described in the reaction mechanism required two-electron transfer processes and were practically the same that detected in part (b) (Fig. 2). These results were discussed and accepted by the literature [27].

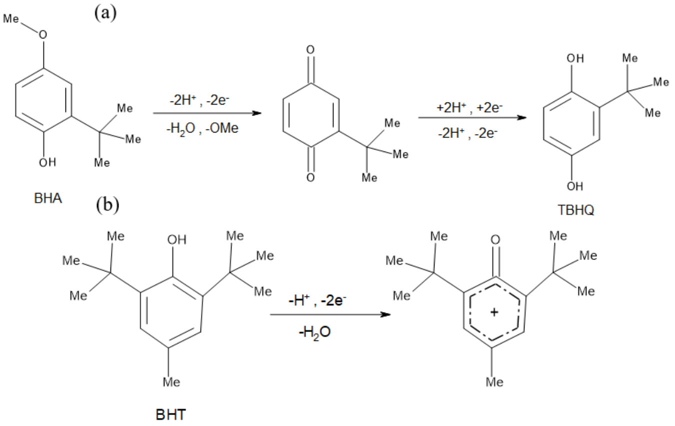

Fig. 2. The electrochemical reaction: (*a*) the oxidation mechanism of BHA and TBHQ at a CPE, (b) the oxidation mechanism of BHT at a CPE

Methods

DPV experiments were carried out in a Micro Autolab system with Potentiostat/Galvanostat device that connected to the computer. The system was set to run through the PC by GPES program. Electrochemical workstation was fabricated regarding with a standard three-electrode Metrohm Model cell.

A conventional electrodes cell assembly consisting of a CPE as a working electrode, platinum wire as an auxiliary electrode, and Ag/AgCl in 3mol/L KCl as a reference electrode. A pH-meter (Hanna pH = 211) that can measure the pH of the solutions was used. A cell stand (Model BAS-C1A) was designed to use the voltammetric scan. Also, the antioxidants solution was stirred between the pre-concentration and analysis steps.

Preparation of iron gall ink

We are prepared iron gall ink by mixing solutions of historically proven gum Arabic as the stabilizer, green vitriol (iron (II) sulfate), and chemically pure raw oak galls with concentrations in a volume ratio of 1:2:3 and 60mL water [28]. A water-soluble ferrous Gallate Complexes is formed through the mixing Gallic with iron sulfate. Due to its solubility, the ink penetrates on the paper surface too deeply, which is not possible to erase. Exposure to air, the ferrous gallate reacts with oxygen and leads to the formation of ferric Gallate pigment. This non-water-soluble complex, defined as a writing ink contributing to its indelibility. Besides the differences in the "oxidation stability" of iron gall inks, we focused on the oxidation reaction parameters. Figure 3 schematically illustrates the various stages of the experiment [29].

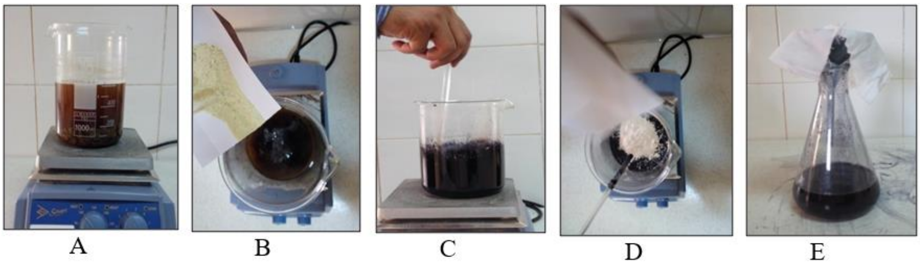

Fig. 3. How to make iron gal ink: A. Boiling the oak gall in water; B. Adding green vitriol; C. Stir the iron and gall; D. Add Arabic gum and mix; E. Composite hardening

Preparation of carbon paste electrode

The carbon paste was prepared by quite mixing of 1.8mL paraffin oil with 5g of graphite powder in a mortar with a pestle for 40min until an identical-wetted paste was obtained. The carbon paste was placed into the hole of the tube and then plunged in the supporting electrolyte placed in the cell. A new carbon paste surface was obtained pushing a by excessive paste out of the tube and polishing with paper [30].

Procedure of electrochemical experiments

The possibilities of the DPV application in antioxidants determination were examined. Generally, measuring the peak current depended on antioxidant concentration. Hence, studies on the quantitative determination of BHA, BHT, and TBHQ in “corrosion Phenomenon” were started with control assays. Furthermore, in the present work, ethanol buffer recommended for the best performance with respect to sensitivity and sharper response. Hence, in first step, a 10mL ethanol buffer solution 0.04M was inserted into the voltammetry cell and then 0.1g of the iron gall ink solution was added into the cell and mixed together. This mixed solution used as a "supporting electrolyte".

Then, the capacity of an antioxidant in corrosion inhibition was evaluated as followed. At first, 30mL of the solution containing intended antioxidant with an initial concentration of 300μM was added to the supporting electrolyte and then stirred for 20min and waited. Results were obtained by DPV method and then the electrodes washed three times with distilled water and ethyl alcohol [31].

Experimental design and Mathematical model

One of the most often design was observed for experiments with mixtures of *q* variable consisting of all possible subsets in the simplex-centroid design (Fig. 4) comprises the $2^q–1$ point (here, will be applied to the three components (TBHQ, BHT, and BHA), where *q* is equal to the sum 1 or 100%. The function used was equation 1 [32]:

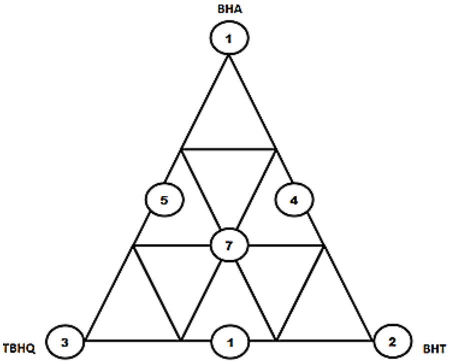

Fig. 4. Simplex-centroid experimental design for BHA, BHT, and TBHQ [29]

The regression equation was determined in optimized conditions.

$$Y(x) = \sum_{1 \le i \le q}^{q} \beta_i x_i + \sum_{1 \le i \le j \le q}^{q} \beta_{ij} x_i x_j + \sum_{1 \le i \le j \le l \le q}^{q} \beta_{ijl} x_i x_j x_l \qquad (1)$$

where:

Y: Response function of *Ea* (kJ·mol^{-1}),
x_1, x_2 and x_3: Ratios of TBHQ, BHT, and BHA in the mixture,
β: Estimated parameters.

Determination of induction period (IP) *and oxidation stability parameters*

"Oxidation Stability" test investigates the antioxidants stability at the long time, were carried out at temperatures of 125, 120, 115, and 110°C. The oxidation stability is characterized by the induction period. Induction period (IP) is calculated by variation of electrical conductance on the plot of conductivity (µS·cm^{-1}) *vs.* time (s) [33, 34]. Hence, Data of the conductivity *vs.* time, determined for all mixtures and temperatures.

Calculation of the oxidation reaction and its kinetic and thermodynamic parameters

The rate constants (*k*) could be determined using the slope of the line in first-order reactions. According to this principle, the kinetic parameters of reaction such as activation energy (*Ea*) and pre-exponential factor (*A*) was obtained by the Arrhenius equation, while the thermodynamic parameters were calculated by the activated complex theory (ACT).

Results and discussion

Differential pulse voltammetry study of gall ink

In order to exact determination of antioxidant, effect of various conditions such as supporting electrolytes, pH, pulse amplitude, oxidation potential and scan rate on the peak current were obtained.

In order to establish the optimum conditions, the DPV technique was both recorded by scanning from 0 to 1.4V with scan rate of 20mV·s^{-1}, and pulse amplitude of 8mV. In addition, experiments were studied at room temperature. At first, the pH value selected in the range of 2-3 and then for quantitative analysis, the scan peak of iron gall ink was studied. As can be seen in Figure 5, the oxidation peaks of iron gall ink were well-defined and stand on between 1.4 to 1.6V.

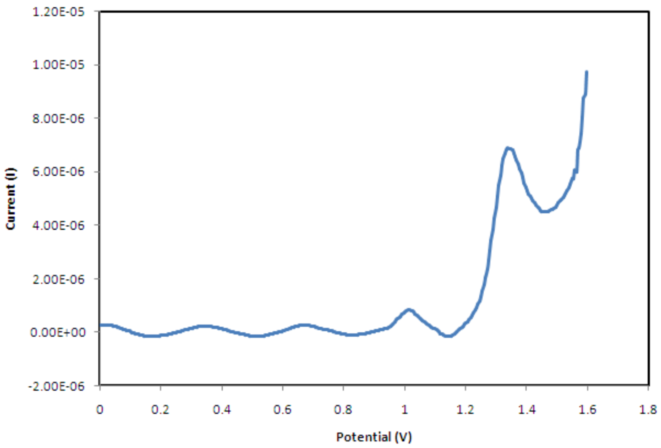

Fig. 5. Quantitative analysis of iron gall ink with scan peak

Linear calibration plots for individual antioxidant

The Calibration graph in the bio-analytical method predicts the relationship between concentration and detected response on least-squares linear regression. From the standards voltammograms, linear calibration plots were obtained.

Calibrations were conducted based on DPV curves of BHA, BHT, and TBHQ oxidation on CPE electrode (based on S/N = 3) between 0.1-12mg/L for TBHQ and 1.2-136mg/L for BHA and BHT (Fig. 6). The peak potentials characteristic indicates all the stability features of BH, BHT, and TBHQ in the linear ranges of the calibration curve.

Therefore, in order to select the optimum concentration of each of the antioxidants, which points precisely on the antioxidant calibration line (BHA: 20, 50 and 100mg/L; BHT: 10, 50 and 65mg/L; TBHQ; 5, 10 and 25mg/L), were selected to perform the electrochemical process.

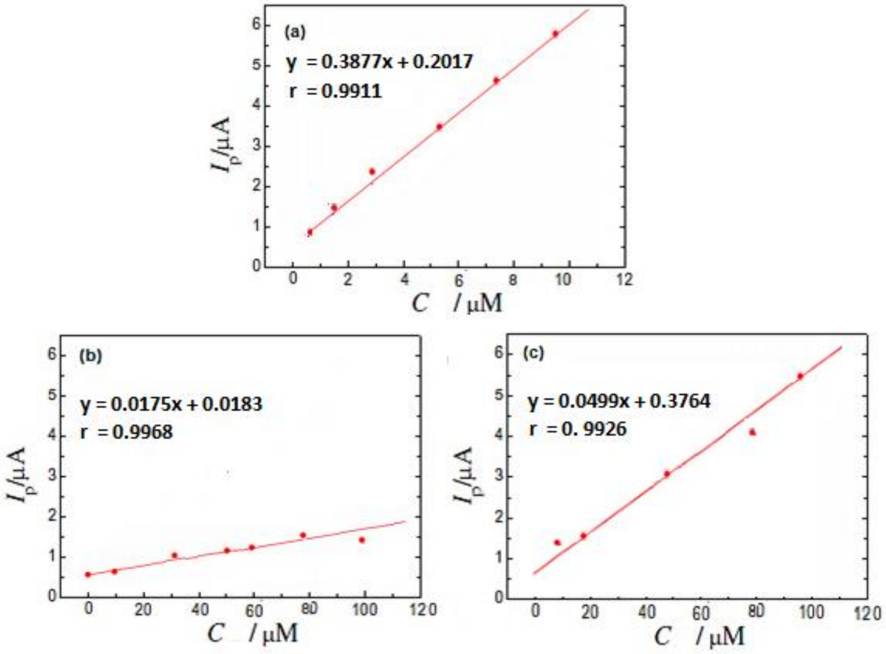

Fig. 6. Linear calibration plots for (*a*) TBHQ, (b) BHT and (c) BHA in individual antioxidant

Differential pulse voltammetry study of antioxidant

Quantitative determination of individual antioxidants was performed according to an earlier reported. Hence, suitable amounts of antioxidant solution containing one of the three antioxidants (BHA, BHT, and TBHQ), were transferred to the electrochemical cell that before filled supporting electrolyte and diluted to 10mL distilled water. Measurements were performed in the three-electrode cell system. All determinations were repeated three times. Characteristic of DPV curve for antioxidants are identically shaped (not shown).

BHA *antioxidant*

The solution of BHA in concentration of 20mg/L was used. Solutions concentrations were calculated with use from their corresponding calibration curve. Figure 7*a*-d presents the typical response of the oxidation of BHA obtained at a CPE. It should be noted that notable no changes in the peak potentials range of concentration curves were observed.

Results demonstrated that the oxidation peak at about 0.54-0.555V can be related to the oxidation of BHA. Generally, the optimum peak current of BHA for their quantitative determination, should be in the range of 540 - 555mV. Then, the solutions of BHA with concentration of 50mg/L and 100mg/L were selected and used. In case of 50 mg/L BHA antioxidant, with increasing concentration of the antioxidant, the increased peak current is seen.

The peak current reached the maximum value (5.64×10^6A) when BHA potential was about 550V; while, in comparison with the previous solutions, in case of 100mg/L BHA antioxidant, with an increase in the concentration of BHA, no change was observed in maximum value of peak current. Therefore, the concentration of 50mg/L of BHA antioxidant is selected as the optimum concentration.

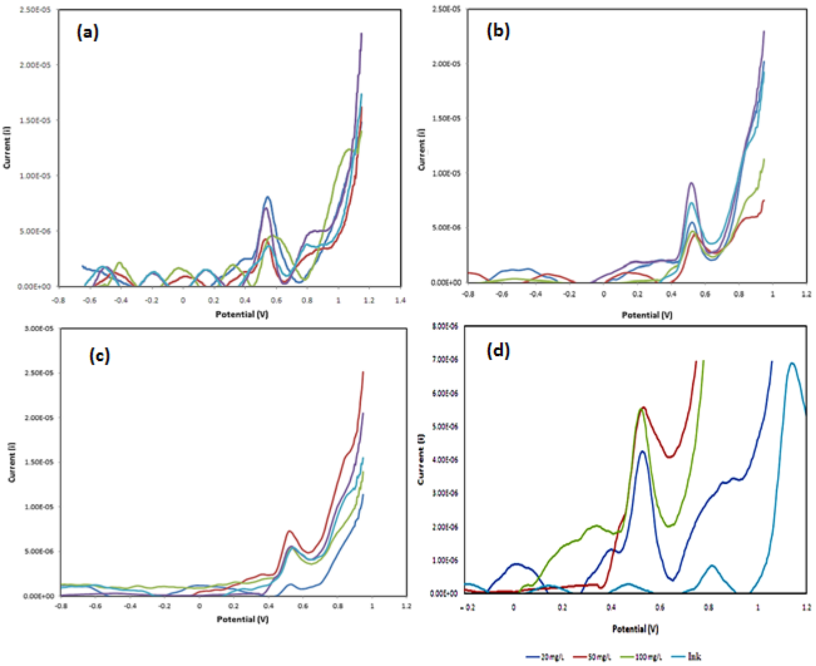

Fig. 7. Typical differential pulse voltammograms of the oxidation of BHA obtained at a CPE: (*a*) 20mg/L, (b) 50mg/L, (c) 100mg/L (d) Overlapping graphs

BHT *antioxidant*

As mentioned above, the solution of BHT in concentration of 10mg/L was used. As can be seen, Figure 8*a*-d demonstrates a model of the oxidation of BHT obtained at a CPE and the peak attributed to BHT oxidation at a potential of 736-790mV can be easily identified. Then, the solutions of BHT in concentration of 50mg/L and 65mg/L were selected and used and peak current increases with increase in the concentration of antioxidant. Therefore, the concentration of 65mg/L of BHT antioxidant is selected as the optimum concentration.

TBHQ *antioxidant*

Firstly, the solution of TBHQ in concentration of 5 mg/L was prepared. Figure 9*a*-d revealed particular diagram of the oxidation of TBHQ obtained at a CPE. Voltammograms show a single peak at a well-defined potential of 362-365mV attributed to oxidation of TBHQ.

Then, the solutions of TBHQ in concentration of 10mg/L and 25mg/L were selected and used. It can be observed that the effect of an increase in peak current and concentration was similarly. Therefore, the concentration of 25mg/L of TBHQ antioxidant is selected as the optimum concentration.

In all of DPV voltagramm of antioxidants, after absorption of antioxidant onto iron gall ink, the maximum peak potential was shifted to a more negative potential with the addition of the antioxidant, indicated that less iron gall ink will be oxidized. In other words, the desired antioxidants (BHA, BHT, and TBHQ) may be able to prevent the oxidation and corrosion of the iron gall ink in documents [35].

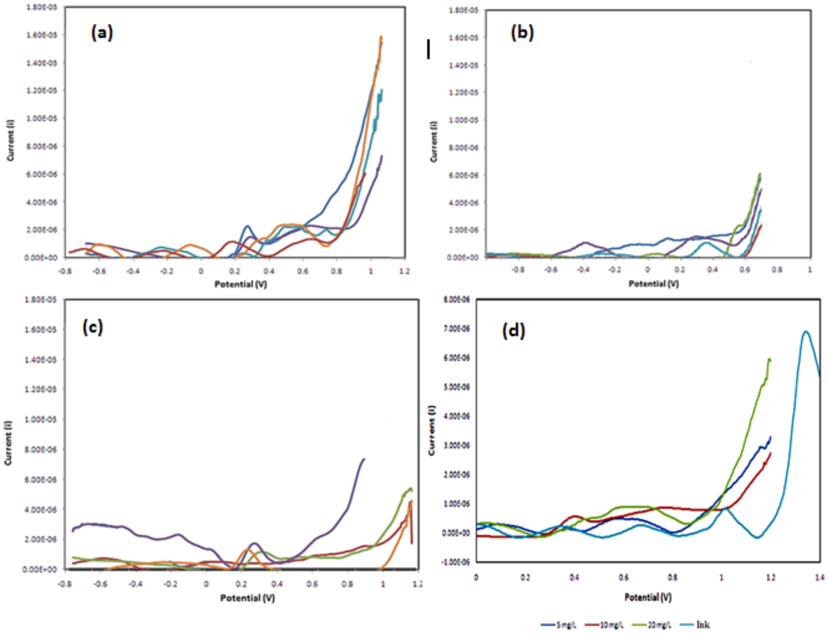

Fig. 8. Typical differential pulse voltammograms of the oxidation of BHT obtained at a CPE: (*a*) 10 mg/L, (b) 50 mg/L, (c) 65 mg/L (d) Overlapping graphs.

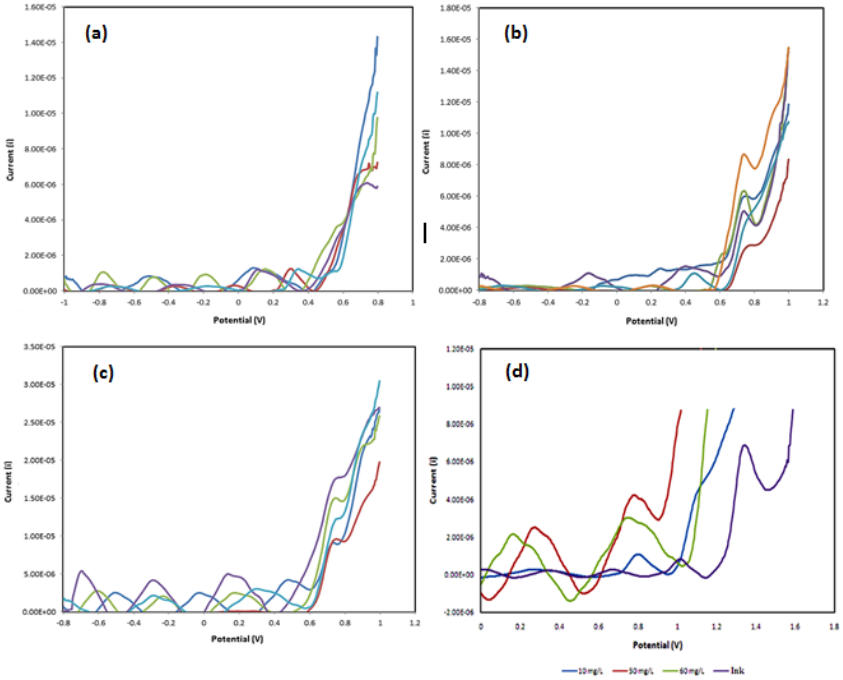

Fig. 9. Typical differential pulse voltammograms of the oxidation of TBHQ obtained at a CPE: (*a*) 5mg/L, (b) 10mg/L, (c) 25mg/L (d) Overlapping graphs

Differential pulse voltammetry study of antioxidants

After qualitative analysis of the antioxidants, the result of diagrams was investigated. It can be seen that the peaks related to oxidation of each of antioxidant can be easily identified. In this voltagramm, three oxidation peaks at approximately of 540-555mV, 736-790mV, and 362-365mV was observed, which this is similar to the oxidation peak was demonstrated for individual antioxidant, previously.

Electrochemical methods including voltammetric standards techniques allowed determining the calibration curve and applying them to the analytical approaches and parameters.

Linear calibration plots for ternary mixture antioxidants

Under the optimized conditions, calibration graphs for ternary mixture antioxidants solution were obtained. This method is characterized by the fact of low limits of detection (LOD), wide linearity range, and limits of quantification (LOQ). Results showed that calibration versus concentration plots for each of antioxidant (BHA, BHT, or TBHQ) based on S/N = 3, were linear in the concentration ranges of, 1.2–100g·mL^{-1}, 1.2–100g·mL^{-1} and 0.1–10g·mL^{-1}, respectively. Therefore, a ternary mixture of BHA, BHT, and TBHQ antioxidant detecting a greatest linear calibration range and lowest limit of detection compared to the standard system (Fig. 10).

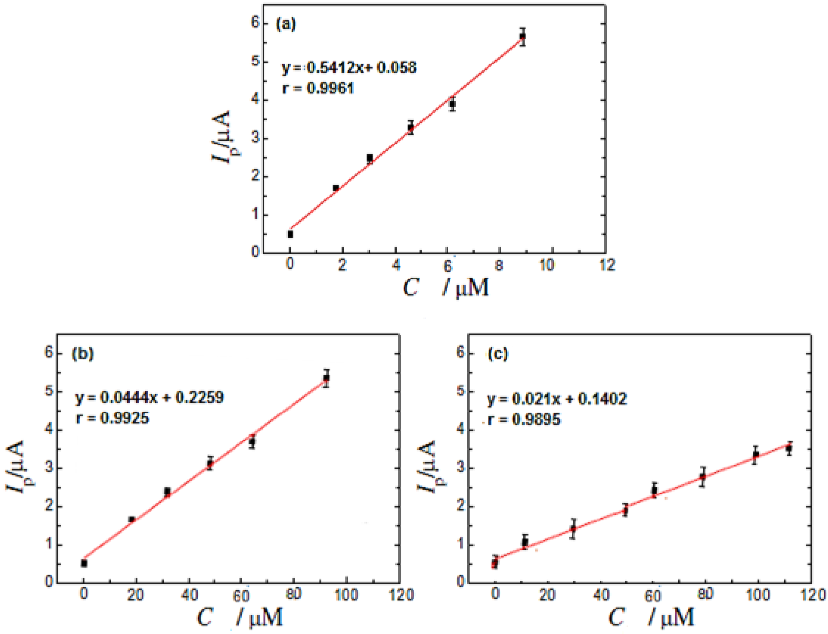

Fig 10. The analytical parameters for the calibration graph in ternary antioxidant

Comparison of calibration curve, limit of quantitation and limit of detection

LOD and LOQ explain the smallest concentration of a measure and that can be calculated by an analytical procedure. Also, R-squared (R^2) describes the ratio of the variance for a dependent variable that's in a regression model obtained by independent variables. Sensitivity measures the proportion of actual positives that are correctly identified. The electrochemical behaviour and the antioxidant effectiveness of BHA, BHT, TBHQ antioxidants and also their ternary mixtures were evaluated by means of DPV, with a view to the prediction of a potential pro-oxidant or synergistic behaviour of mixtures of antioxidants [36, 37]. For the calibration graph, the analytical parameters values (LOD, LOQ, R^2, and sensivity) are mentioned in Table 1.

Table 1. Linear regression analysis and limit of detection by DPV for the quantification of individual and ternary mixture of antioxidant

Process	antioxidant	(R^2)	LDR ($\mu molL^{-1}$)	LOD ($\mu molL^{-1}$)	Sensitivity ($\mu A\ \mu molL^{-1}$)
Individual	TBHQ	0.9911	0.1-12	0.015	0.3877
	BHT	0.9968	1.2-136	0.14	0.0175
	BHA	0.9926	1.2-136	0.14	0.0499
Ternary	TBHQ	0.9961	0.1-10	0.015	0.5412
	BHT	0.9925	1.2-100	0.14	0.0210
	BHA	0.9895	1.2-100	0.14	0.0444

As stated earlier, results obtained from Table 1 showed that a ternary mixture of BHA, BHT, and TBHQ antioxidant provides a broader linear calibration range and a lower limit of detection. Hence, a ternary combination of antioxidants with relative concentrations predetermined, for example, BHA at a concentration of 0.1% m/m, BHT at a concentration of 0.13% m/m, and TBHQ at a concentration of 0.05% m/m can be used to prevent corrosion of the iron gall ink compounds in the documents. Generally, for each, the values were evaluated based on previous research and of oxidative stability tests.

Oxidation stability at different temperatures

Oxidation stability is an important quality parameter for antioxidants. Possible interaction effects between BHA, BHT, and TBHQ were evaluated by employing a (2^3-1) factorial design. According to Table 2, it can be seen that BHT demonstrated the lowest values of I_P in all treatments. Generally, IP values increased with decreasing temperature and adding antioxidants.

As a result, efficiency of single antioxidants, arrange by TBHQ, BHA and BHT, respectively. The high efficacy of TBHQ related to the two *para*-hydroxyl groups in chemical structure, probably. The results showed that the best response was attained in the mixture comprising TBHQ and BHT antioxidants.

Table 2. IP values at different temperatures for each test from simplex centroid mixture design.

Treatment	Mixture (TBHQ, BHT, BHA)	Ip/h			
		125ºC	120ºC	115ºC	110ºC
1	(1, 0, 0)	1.87	2.19	3.22	6.23
2	(0, 1, 0)	0.69	1.24	2.23	3.64
3	(0, 0, 1)	1.62	2.19	3.10	5.62
4	(½, ½, 0)	1.34	2.27	3.44	5.56
5	(½, 0, ½)	1.58	1.95	2.68	7.52
6	(0, ½, ½)	1.66	1.89	2.67	4.18
7	(1/3, 1/3, 1/3)	1.28	1.99	2.65	5.77

Kinetics and thermodynamics of the oxidation reaction at different temperatures

The rate constant as indicated in the equation by the letter *k*. Table 3 introduces the average values of rate constants (*k*), calculated by the following formula.

$$ln\,\Lambda_0 = k\left(t_f - t_i\right) + \ln\Lambda \tag{2}$$

where: *k*: Rate constant (h^{-1}), t_f: Final time (s), t_i: Initial time (s).

In Table 3, the values of the rate constants decrease, by the presence of antioxidants. The k value is attributed to the molecular structures of antioxidants, and only BHT (treatment 2) revealed the highest K-values, compared with other antioxidants and followed by mixture comprising TBHQ, BHA, and BHT.

Table 3. Rate constants (*k*) at different temperatures for all treatments

Treatment	Mixture (TBHQ, BHT BHA)	k / h^{-1} 125 ºC	 120 ºC	 115 ºC	 110 ºC
1	(1, 0, 0)	1.548	1.218	0.9197	0.5523
2	(0, 1, 0)	2.112	1.809	1.340	0.9251
3	(0, 0, 1)	1.465	1.291	0.9227	0.5853
4	(½, ½, 0)	1.650	1.178	0.7978	0.4898
5	(½, 0, ½)	1.749	1.193	1.088	0.4585
6	(0, ½, ½)	1.555	1.511	1.150	0.6597
7	(1/3, 1/3, 1/3)	1.8107	1.3590	1.0316	0.5160

However, as a consequence of the decrease in the rate of consumption, the values of *k* decrease with decreasing temperature for all treatments. The obtained results show that the oxidation process is temperature dependent.

Then, kinetic data can be calculated by Arrhenius equation:

$$ln(k) = ln\ A - E_a/RT \tag{3}$$

where: *R*: The ideal gas constant (= 8.31447J·K^{-1}·mol^{-1}), *A*: The pre-exponential factor (h^{-1}), *Ea*: The activation energy (kJ mol^{-1}), T: The absolute temperature (ºK).

The Arrhenius equation is the equation of a straight line whose slope is –E*a*/R. The activated complex theory (ACT) explains the effect of temperature on reaction rate which led to the Eyring equation as described by equation 4:

$$ln(k/T) = [\ln(k_B/h) + (\Delta S^{t}/R) - (\Delta H^{t}/R)(1/T) \tag{4}$$

where: k_B: The Boltzmann constant (1.38×10^{-23}J·K^{-1}), *h*: The Planck's constant (6.62×10^{-34}J·s).

The thermodynamic parameters of the reactions consist of ΔH‡ and Δ*S*‡ are the enthalpy of activation (kJ·mol^{-1}) and the entropy of activation (J·mol^{-1}·K^{-1}), respectively. The symbol ‡ referred to as the activated complex. According to the equation 4, for determination of ΔH‡ and Δ*S*‡, a plot of *ln k/*T *vs. 1*/T (K^{-1}) provided a straight line with slope (–ΔH‡/*R*) and intercept [*ln* $(k_B/h) + (\Delta S‡/R)$].

The activation energy describes and explains the effect of changing the temperature on the reactions. The exponential relationship between rate and E*a* means that in higher values of E*a*, small changes in temperature result in large changes in the oxidation rate.

Consequently, the reaction rate is much slower at the lower E*a* and is relatively independent of temperature.

The values of *Ea* are illustrated in Table 4, where the sample of pure BHT showed the lowest value and as it follows, the mixture treatments including BHA and BHT showed greater values of E*a*. Also, In the case of antioxidants mixture, TBHQ and BHA showed the highest value of *Ea*. The significant antioxidant synergism, between three different antioxidants, was observed for ternary mixtures of antioxidants.

Due to the E*a* value for each mixture of antioxidants greater than the sum of E*a* value for the individual antioxidant. In Table 4, there is considerable evidence that BHT and BHA displayed no evidence of any positive synergic effect that would justify their use in binary mixtures which showed the lowest value between these mixtures. In all treatment, ΔH‡ values are positive. Moreover, the addition of TBHQ antioxidants to mixtures seemed to increase ΔH‡ values through synergism with another antioxidant. This observed effect was reported in the presence of BHA and BHT antioxidants.

Table 4. Kinetic and thermodynamic parameters for oxidation

Treatment	Thermodynamics			Kinetics	
	ΔG‡ (kJ·mol^{-1})	ΔS‡ (J·K^{-1}·mol^{-1})	ΔH‡ (kJ·mol^{-1})	A (h^{-1})	E*a* (kJ·mol^{-1})
1	96.54	–36.20	82.40	2.84×10^{11}	85.65
2	95.26	–71.22	67.44	4.21×10^{9}	70.68
3	96.50	–54.42	75.24	3.18×10^{10}	78.48
4	96.72	6.07	99.09	4.58×10^{13}	102.33
5	96.47	12.08	101.19	9.45×10^{13}	104.43
6	96.04	–68.69	69.21	5.71×10^{9}	72.46
7	96.28	8.13	99.46	5.88×10^{13}	102.70

Moreover, the higher of entropy of activation (Δ*S*‡) showed a greater resistance to oxidation. I should say that, with increasing or decreasing the degrees of freedom, ΔS‡ is going to get a positive and negative value, respectively. On the other hand, the Gibbs frees energy of activation (ΔG‡) was determined by the fundamental thermodynamic equation:

$$\Delta G^{\ddagger} = \Delta H^{\ddagger} - T\Delta S^{\ddagger} \tag{5}$$

In Table 4, all samples revealed positive values of ΔG‡, which means that they will be non-spontaneous. It can also be mentioned that all of the treatments show a decrease in temperature and reaction rate with an increase in ΔG‡.

Conclusions

The differential pulse voltammetric technique permits the successful quantitation of the electrochemical methods applied to BHA, BHT, and TBHQ antioxidant activity. In This paper, the electrochemical behaviors of the three antioxidants at the proposed procedure were inquired, and it was demonstrated that the carbon paste electrode presented clear advantages as a renewable electrode surface. Furthermore, the calibration curves plotted for the simultaneous determination of a ternary mixture of antioxidants were validated. More results demonstrated that combining kinetics and thermodynamics parameters with analysis of experimental design and mathematical model provides opportunities that may help to improve the viable alternative systems for the future. This method is less expensive than other techniques and can be applied to the quantitative determination of the ink corrosion.

Acknowledgments

Support of this investigation by Art University of Isfahan is gratefully acknowledged.

Conflict of interest

The authors certify that they have NO affiliations with or involvement in any organization or entity with any financial interest or non-financial interest in the subject matter or materials discussed in this manuscript.

References

[1] M. Afsharpour, S. Imani, *Preventive protection of paper works by using nanocomposite coating of zinc oxide*, **Journal of Cultural Heritage, 25**, 2017, pp. 142–148.

[2] A.A. Ariafar, M. Afsharpour, K. Samanian, *Use of TiO_2/chitosan nanoparticles for enhancing the preservative effects of carboxymethyl cellulose in paper-art - works against Biodeterioration,* **International Biodeterioration Biodegradation, 131**, 2018, pp. 67-77.

[3] A. Gimat, A.L. Dupont, H. Lauron-Pernot, S. Paris, V. Rouchon, P. Massiani, *Behavior of cellobiose in iron-containing solutions: towards a better understanding of the dominant mechanism of degradation of cellulosic paper by iron gall inks,* **Cellulose, 24**, 2017, pp.5101-5115.

[4] Y. Liu, I.K. Cigi, M. Strlic, *Kinetics of accelerated degradation of historic iron gall ink-containing paper,* **Polymer Degradation and Stability, 142**, 2017, pp. 255-262.

[5] M. Afsharpour, M. Haddadi, *Titanium dioxide thin film: environmental control for preservation of paper-artworks,* **Journal of Cultural Heritage**, **15**, 2014, pp. 569–574.

[6] M. Afsharpour, F.T. Rad, H. Malekian, *New cellulosic titanium dioxide nanocom-posite as a protective coating for preserving paper-artworks*, **Journal of Cultural Heritage**, **12**, 2011, pp. 380–383.

[7] C. Krekel, *Chemistry of historical iron gall inks,* **International Journal of Forensic Document Examiners, 5**, 1999, pp.54-58.

[8] R.J.D. Hidalgo, R. Córdoba, P. Nabais, V. Silva, M.J. Melo, F. Pina, N. Teixeira, V. Freitas, *New insights into iron-gall inks through the use of historically accurate reconstructions*, **Heritage Science, 6,** 2018, Article Number: 63.

[9] A. Potthast, U. Henniges, G. Banik, *Iron gall ink-induced corrosion of cellulose: aging, degradation and stabilization. Part 1: model paper studies,* **Cellulose**, **15**, 2008, pp. 849–859.

[10] U. Henniges, R. Reibke, G. Banik, E. Huhsmann, U. Hahner, T. Prohaska, A. Potthast, *Iron gall ink-induced corrosion of cellulose: aging, degradation and stabilization. Part 2; Application on historic sample material,* **Cellulose**, **15**, 2008, pp. 861-870.

[11] G.P. Junior, B. Reibland, *Risk assessment: A tool to compare alternative courses of action for the conservation of iron-gall ink containing objects,* **Restaurator**, **24**, 2003, pp. 205-226.

[12] J. Kosek, C. Barry, *Investigating the condition of iron gall ink drawings: developing an assessment survey,* **Journal of the Institute of Conservation**, **42**, 2019, pp. 191-209.

[13] M. Boutiuc, O. Florescu, V. Vasilache, I. Sandu, *The Comparative Study of the State of Conservation of Two Medieval Documents on Parchment from Different Historical Periods,* **Materials, 13**(21), 2020, Article Number: 4766, DOI10.3390/ma13214766.

[14] O. Florescu, R. Hritac, M. Haulica, I. Sandu, I. Stanculescu, V. Vasilache, *Determination of the Conservation State of Some Documents Written on Cellulosic Support in the Poni-Cernatescu Museum, Iasi City in Romania,* **Applied Sciences-Basel, 11**(18), 2021, Article Number: 8726, DOI10.3390/app11188726.

[15] B. Reisslands., *Visible progress of paper degradation caused by Iron Gall inks*, **The iron gall ink meeting**, Newcastle, 2001.

[16] J. Kolar, M. Strlic, M. Budnar, J. Malesic, V.S. Selih, J. Simcic, *Stabilization of Corrosive Iron Gall Inks,* **Acta Chimica Slovenica, 50**, 2003, pp. 763-770.

[17] J. Kolar, M. Sala, M. Strlic, V.S. Selih, *Stabilisation of paper containing iron-gall ink with current aqueous processes.* **Restaurator**, **26**, 2005, pp. 181-189.

[18] M.J. Jeong, A.L. Dupont, E.R. de la Rie, *Degradation of cellulose at the wet–dry interface. II. Study of oxidation reactions and effect of antioxidants,* **Carbohydrate Polymers, 101**, 2014, pp. 6 71–683.

[19] J. Kolar, A. Mozir, V. Balazzo, T. Steemers, G. de Bruin, *New Antioxidants for Treatment of Transition Metal Containing Inks and Pigments,* **Restaurator, 29**, 2008, pp. 84-198.

[20] D. Mills, *Electrochemical Methods in Corrosion Research,* **The International Journal of Corrosion Processes and Corrosion Control**, **42**, 2007, pp. 12-13.

[21] Y. Youngmi, G. Weinberg, M. Prenzel, M. Greiner, S. Heumann, S. Becker, R. Schlögl, *Electrochemical corrosion of a glassy carbon electrode,* **Catalysis Today**, **295**, 2017, pp. 32-40.

[22] B. Kanngieger, O. Hahn, M. Wilke, B. Nekat, W. Malzer, A. Erko, *Investigation of oxidation and migration processes of inorganic compounds in ink-corroded manuscripts,* **Spectrochimica Acta**, **Part B: Atomic Spectroscopy, 59**, 2004, pp. 1511-1516.

[23] R.P. Caramit, A.G. de Freitas Andrade, J.B.G. de Souza, T.A. de Araujo, L.H. Viana, M.A.G. Trindade, V.S. Ferreira, *A new voltammetric method for the simultaneous determination of the antioxidants TBHQ and BHA in biodiesel using multi-walled carbon nanotube screen-printed electrodes,* **Fuel**, **105**, 2013, pp. 306–313.

[24] G. Banik, *Scientific conservation: Transfer of scientific research on ink corrosion to conservation practice – does it take place?* **Restaurator**, **30**, 2009, pp. 131–146.

[25] F. Andreatta, L. Fedrizzi, *The use of the electrochemical micro-cell for the investigation of corrosion phenomena*, **Electrochimica Acta**, **203**, 2016, pp. 337-349.

[26] J. Pokorný, *Natural antioxidants for food use,* **Trends in Food Science & Technology, 2**, 1991, pp. 223-227.

[27] X. Lin, Y. Ni, S. Kokot, *Glassy carbon electrodes modified with gold nanoparticles for the simultaneous determination of three food antioxidants,* **Analytica Chimica Acta**, **765**, 2013, pp. 54-62.

[28] S. Zekrgoo, *Methods of Creating, Testing and Identifying Traditional Black Persian Inks,* **Restaurator**, **35**, 2014, pp. 133-158.

[29] D. Merli, A. Profumo, C. Dossi, *An analytical method for Fe(II) and Fe(III) determination in pharmaceutical grade iron sucrose complex and sodium ferric gluconate complex,* **Journal of Pharmaceutical Analysis, 2**, 2012, pp. 450–453.

[30] M. Sadeghi, M. Jahanshahi, H. Javadian, *Highly sensitive biosensor for detection of DNA nucleobases: Enhanced electrochemical sensing based on polyaniline/single-layer* MoS_2 *nanosheetsnanocomposite modified carbon paste electrode,* **Microchemical Journal**, **152**, 2020, Article Number: 104315.

[31] Y. Xiang, X. Qian, M. Hua, B Cheng, W. Chen, J. Li, *Voltammetric Determination of Dinonyl Diphenylamine and ButylatedHydroxytoluene in Mineral and Synthetic Oil,* **Analytical Letters, 49**, 2016, pp.1526-1536.

[32] M.S. Raymundoa, M.M.S. Paulab, C. Francoc, R. Fett, *Quantitative determination of the phenolic antioxidants using voltammetric techniques,* **LWT-Food Science and Technology**, **40**, 2007, pp. 1133-1139.

[33] B.D. Ãsio, G. Diego, P. Jaqueline, O. Juliane, A. Karina, C. Rodolfo, *Kinetic and Thermodynamic Parameters of Biodiesel Oxidation with Synthetic Antioxidants: Simplex Centroid Mixture Design,* **Journal of the Brazilian Chemical Society**, **25**, 2014, pp. 1984-1992.

[34] M. Taghvaei, S.M. Jafari, *Application and stability of natural antioxidants in edible oils in order to substitute synthetic additives,* **Journal of Food Science and Technology, 52**, 2015, pp. 1272–1282.

[35] M. Jablonský, J. Kazíková, S. Holúbková, *The effect of the iron-gall ink on permanence in paper by breaking length, degree of polymerisation and thermogravimetric stability of paper during accelerated ageing,* **Acta Chimica Slovenica, 3**, 2010, pp .63–73.

[36] T.G. Diaz, A.G. Cabanillas, M.F.A. Franco, F. Salinas, J.C. Vire, *Voltammetric Behavior and Simultaneous Determination of the Antioxidants Propyl Gallate, Butylated hydroxyanisole, and Butylated hydroxytoluene in Acidic Acetonitrile-Water Medium Using PLS Calibration,* **Journal of Electroanalytical Chemistry, 10**, 1998, pp. 497-505.

[37] N. Yongnian, L. Wang, S. Kokot, *Voltammetric determination of butylated hydroxyanisole, butylated hydroxytoluene, propylgallate and tertbutyl hydroquinone by use of chemometric approaches,* **Analytica Chimica Acta**, **412**, 2000, pp 185–193.

Received: December 21, 2020
Accepted: January 23, 2022